

A nanomechanical device based on linear molecular motors

Tony Jun Huang, Branden Brough, and Chih-Ming Ho^{a),b)}

Mechanical and Aerospace Engineering Department and the Institute for Cell Mimetic Space Exploration, University of California, 420 Westwood Plaza, Los Angeles, California 90095

Yi Liu, Amar H. Flood, Paul A. Bonvallet, Hsian-Rong Tseng, and J. Fraser Stoddart^{a),c)}

Department of Chemistry and Biochemistry and the California NanoSystems Institute, University of California, 405 Hilgard Avenue, Los Angeles, California 90095-1596

Marko Baller and Sergei Magonov

Veeco Instruments, 112 Robin Hill Road, Santa Barbara, California 93117

(Received 17 June 2004; accepted 19 August 2004)

An array of microcantilever beams, coated with a self-assembled monolayer of bistable, redox-controllable [3]rotaxane molecules, undergoes controllable and reversible bending when it is exposed to chemical oxidants and reductants. Conversely, beams that are coated with a redox-active but mechanically inert control compound do not display the same bending. A series of control experiments and rational assessments preclude the influence of heat, photothermal effects, and pH variation as potential mechanisms of beam bending. Along with a simple calculation from a force balance diagram, these observations support the hypothesis that the cumulative nanoscale movements within surface-bound “molecular muscles” can be harnessed to perform larger-scale mechanical work. © 2004 American Institute of Physics. [DOI: 10.1063/1.1826222]

Nanoscale actuators, capable of converting chemical or electrical energy into mechanical motion, are needed for a wide range of applications. The bottom-up approach, which employs atoms and molecules both as the fundamental building blocks and as the working units, is potentially capable of delivering efficient operations at dramatically reduced scales compared with traditional microscale actuators.^{1–3} While a number of actuating materials have been developed,^{4–6} they rely primarily upon the response of a bulk substance devoid of moving components, and the theoretical descriptions of their operation are still being developed. By contrast, simple molecular components in nature, e.g., myosin and actin in skeletal muscle, can be organized to perform complex mechanical tasks beginning at the nanometer scale but expressed in the macroscopic world. In this letter, we describe an integrated approach that combines the bottom-up assembly of molecular functionality with the top-down manufacture of architectures for the establishment of nano-chemomechanical systems.

Artificial molecular machinery⁷ is an attractive means for performing controllable mechanical work that begins at the nanoscale. Bistable [2]rotaxanes hold particular promise in this regard. They have been likened to linear molecular motors on account of their ring component's ability to undergo controllable mechanical switching between two or more recognition sites located along their linear dumbbell portions⁸ in response to a chemical, electrochemical, or photochemical stimulus.⁹ Recent investigations have established that bistable [2]rotaxanes maintain the same redox-driven mechanical switching whether they are in solution, self-assembled¹⁰ in condensed phases, or mounted¹¹ on solid substrates. Since most mechanical devices rely upon solid supports for the transmission of actuation forces, these re-

sults provide the impetus for the development of nanomechanical devices. In this letter, we describe the nanomechanical response of microcantilever beams coated with a self-assembled monolayer (SAM) of artificial molecular motors following the cycled addition of chemical redox reagents. A simple model that considers the mechanical movements of each molecule within the SAM verifies chemomechanical transduction as a likely mechanism for cantilever bending. We also describe the results of a structure-function study conducted on a control compound along with a series of control experiments and rational assessments to account for a wide range of alternative interaction mechanisms.^{4–6} The data provide compelling evidence for chemomechanical transduction as a general mode of operation for the generation of force from surface-bound linear molecular motors.

Expanding upon a series of bistable [2]rotaxanes,⁸ a bistable [3]rotaxane **R1**⁸⁺ [Fig. 1(a)] was created as a “molecular muscle”¹² to mimic the contraction and extension movements of skeletal muscle. This design takes advantage of well-established recognition chemistry⁸ that selectively positions the cyclobis(paraquat-*p*-phenylene) (CBPQT⁴⁺) rings around the two tetrathiafulvalene (TTF) stations of **R1**⁸⁺, as opposed to the two naphthalene (NP) stations. Chemical oxidation of the TTF stations to their dicationic form (TTF²⁺) drives the CBPQT⁴⁺ rings to the NP stations. This “power stroke” arises primarily from electrostatic charge–charge repulsion between the CBPQT⁴⁺ rings and the TTF²⁺ stations. Upon reduction of the two TTF²⁺ stations back to their neutral form, the inter-ring distance increases as the CBPQT⁴⁺ rings return to the TTF stations by means of a thermally activated “diffusive stroke.” Thus, the cycle of contraction and extension within **R1**⁸⁺ mimics the motion which takes place inside natural muscle fibers. The incorporation of a disulfide tether onto each CBPQT⁴⁺ ring component provides an anchoring point by which the [3]rotaxane can be attached to a gold surface as a SAM.

^{a)}Authors to whom correspondence should be addressed.

^{b)}Electronic mail: chihming@seas.ucla.edu

^{c)}Electronic mail: stoddart@chem.ucla.edu

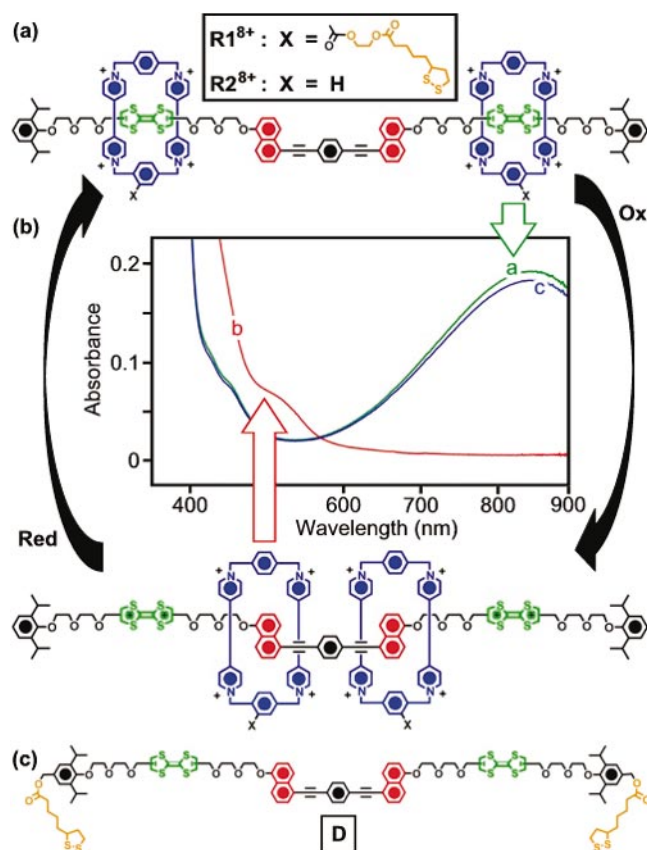


FIG. 1. (Color) (a) Molecular structures and (b) UV/visible absorption spectra of the extended and contracted [3]rotaxanes $\mathbf{R1}^{8+}$ and $\mathbf{R2}^{8+}$. (c) Molecular structure of the disulfide-tethered dumbbell compound \mathbf{D} .

The chemical switching of a simplified derivative $\mathbf{R2}^{8+}$ and its cycle of contraction and extension in solution (MeCN) was confirmed by UV/visible spectroscopy. Its starting state is identified [Fig. 1(a), curve a] by an absorption band at 840 nm that arises⁸ from the charge–transfer (CT) interaction between the TTF stations and the CBPQT⁴⁺ rings. Addition of four equivalents of the oxidant $\text{Fe}(\text{ClO}_4)_3$ caused the appearance of a new band at 510 nm, characteristic [Fig. 1(a), curve b] of the CT transition⁸ between the NP stations and the CBPQT⁴⁺ rings, confirming the movement of both CBPQT⁴⁺ rings from the TTF stations to the NP stations. Introduction of four equivalents of aqueous ascorbic acid as a reductant led to the restoration [Fig. 1(a), curve c] of the original spectrum.

The reversible switching of $\mathbf{R2}^{8+}$ in solution provides a model for its mechanical motion when it is attached to a surface. The persistence of switching in the model [2]rotaxanes on solid substrates^{10,11} supports our expectation that oxidation of $\mathbf{R1}^{8+}$ will generate a tensile stress upon a gold surface through the contractive action of its two disulfide-tethered CBPQT⁴⁺ rings. If the substrate is sufficiently thin and flexible, such as a long cantilever beam, the cumulative effect of each individual “molecular muscle” will produce an upward mechanical bending of the beam. Correspondingly, reduction of the oxidized and contracted $\mathbf{R1}^{12+}$ will return the CBPQT⁴⁺ rings to the TTF stations and consequently relieve the stress upon the beam, resulting in a downward motion and a return to the beam’s equilibrium position.

A single beam’s deflection upon contraction of the “molecular muscle” was analyzed (see EPAPS Ref. 13) using a simple model for the [3]rotaxane $\mathbf{R1}^{8+}$ bound to a section of

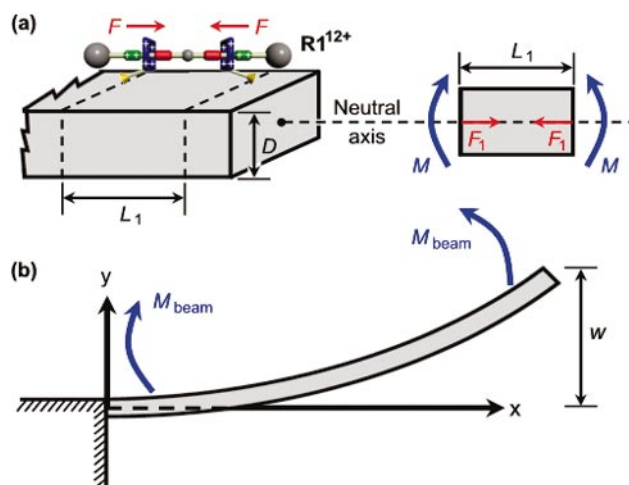


FIG. 2. (Color) Free-body diagrams showing (a) the contractive force F exerted by $\mathbf{R1}^{12+}$ within a single functional unit of the beam along with the associated upward bending moment M and (b) the bending moment M_{beam} for the entire cantilever beam that produces an out-of-plane displacement w .

the beam [Fig. 2(a)]. Oxidation produces a contraction of the inter-ring distance and correspondingly exerts a force F plus a bending moment M upon the beam. Only the sections of the beam between the two moving rings will be subjected to the action of the bending moment M , while the other sections have a zero bending moment. The out-of-plane displacement w of a cantilever beam [Fig. 2(b)] is governed by the Euler–Bernoulli Beam equation,

$$w = \frac{M_{\text{beam}}L^2}{2EI}, \quad (1)$$

in which M_{beam} is the moment on the beam, L is the total length of the cantilever beam, E is the Young’s modulus of the cantilever, and I is the area moment of inertia of the beam’s cross section. The parameter M_{beam} can be obtained by assuming that the force generated (40 pN) by a single molecule¹³ is solely due to electrostatic effects ($\epsilon_{\text{water}}=80$), the SAM covers 100% of the gold surface, and the molecules are idealized as randomly oriented noninteracting rigid rods. Based on this simplified model, the force generated by the “molecular muscle” can act against the spring-like restoring force of a cantilever beam ($500 \times 100 \times 1 \mu\text{m}$) to produce a theoretical beam displacement w of 48 nm.¹³

This chemomechanical design was tested with a gold-coated silicon cantilever array that was coated with a SAM of $\mathbf{R1}^{8+}$ [Fig. 3(a)] and placed in a transparent fluid cell. The position of each cantilever beam was monitored by an optical lever on a Digital Instruments Scentris™ platform while aqueous $\text{Fe}(\text{ClO}_4)_3$ (oxidant) and ascorbic acid (reductant) solutions were sequentially introduced into the fluid cell. Addition of the oxidant solution caused the cantilever beams to bend upward by ~ 35 nm to an apparent saturation point [Fig. 3(b), top series of traces]. Entry of the reductant solution caused the beams to bend back downward to their starting positions. This behavior was observed for all four cantilever beams for 25 cycles (the first three complete cycles are shown here). The slight attenuation in beam deflection following each cycle is attributed to a gradual chemical and/or physical passivation¹⁴ of the SAM. Nevertheless, the movement of the cantilever beams is directly correlated with the cycling of the oxidant and reductant solutions and the experi-

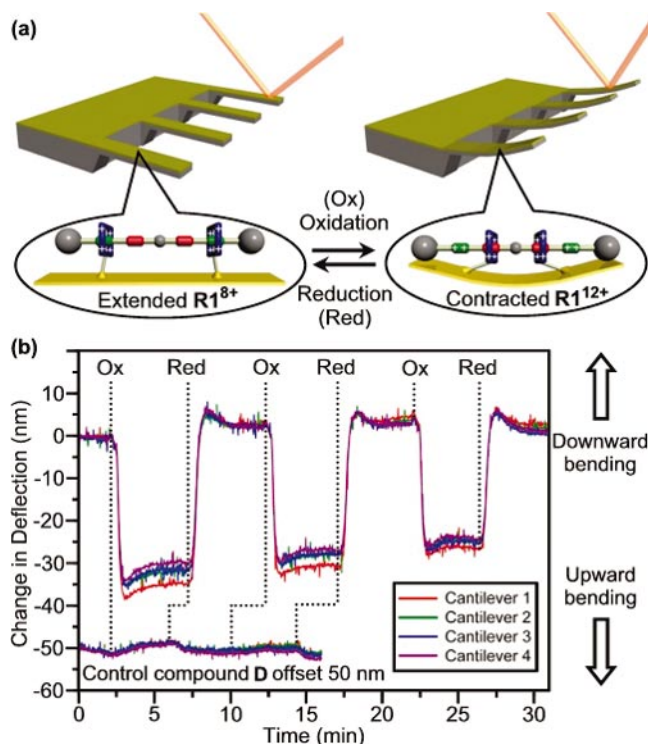


FIG. 3. (Color) Schematic diagram (a) of the proposed mechanism of the device's operation. The experimental data (b) show bending of the four cantilever beams, as the aqueous oxidant (Ox) and reductant (Red) solutions are delivered to the sample cell. A negative deflection corresponds to an upward bending of the cantilever beams. The top series of traces shows the deflection of the cantilever array coated with $\mathbf{R1}^{8+}$, while the bottom series of traces (offset by 50 nm) shows the limited movement of the cantilever array coated with the dumbbell control compound \mathbf{D} .

mental data (35 nm displacement) match closely with the theoretical quantitative analysis (48 nm displacement).

In order to assert that the beams' bending is not a consequence of mundane conformational and/or electrostatic changes within the semirigid $\mathbf{R1}^{8+}$ backbone, the disulfide-tethered dumbbell compound \mathbf{D} [Fig. 1(b)] was synthesized. This control compound contains pairs of TTF and NP recognition sites with the same relative geometries as are present in $\mathbf{R1}^{8+}$. However, \mathbf{D} lacks the mechanically mobile CBPQT $^{4+}$ rings and the disulfide tethers are attached at different locations on the dumbbell's two stoppers. An array of cantilever beams coated with a SAM of \mathbf{D} bends only slightly [Fig. 3(b), bottom series of traces] following sequential injections of the same oxidant and reductant solutions used to study $\mathbf{R1}^{8+}$. This observation suggests that the presence of the mechanically active, disulfide-tethered CBPQT $^{4+}$ rings in $\mathbf{R1}^{8+}$ are essential for the redox-controlled bending of the cantilever beams. The direction of these slight deflections, consistent with electrostatic charge repulsion, is contrary (downward upon oxidation) to that observed in the bending of the beams coated with $\mathbf{R1}^{8+}$. Likewise, thermal and photothermal effects would also bend the bimorph beams downward upon oxidation, but are negligible due to the high heat capacity of water. Further control experiments with $\mathbf{R1}^{8+}$ verify that pH variations within the range of the redox agents do not bend the beams.¹³ Given that all these factors do not contribute to a concerted motion of the canti-

lever, the deflection of the beams coated with a SAM of $\mathbf{R1}^{8+}$ is consistent with our chemomechanical transduction hypothesis. This result suggests that the cumulative effect of individual molecular-scale motions within the disulfide-tethered [3]rotaxane molecules, even when randomly aligned, can be harnessed to perform larger-scale mechanical work.

In summary, a hybrid top-down/bottom-up approach has been employed to create a molecular machine-based actuator that displays reversible bending through the cycled addition of aqueous oxidant and reductant solutions. The bending is assigned to the same chemically driven mechanical contraction and extension of the inter-ring distance observed in a model bistable redox-controllable [3]rotaxane in solution. This phenomenological correlation is supported by control experiments and a theoretical model that accounts for the bending based on the force produced by surface-bound, bistable, redox-controllable [3]rotaxane molecules. Although challenges remain, including the development of direct electrical or optical stimulation, the technological foundation for the production of a class of multiscale nanomechanical devices ultimately to be based upon optimized molecular mechanical motions appears to have been laid.

The authors gratefully acknowledge B. Northrop, S. Solares, U. Ulmanella, X. Zhang, W. Klug, N. Fang, C. Prater, M. Blanco, and S.-T. Lin for valuable discussions and technical assistance. This work was supported in part by the National Science Foundation, the Defense Advanced Research Projects Agency, and NASA's Institute for Cell Mimetic Space Exploration.

¹M. Madou, *Fundamentals of Microfabrication* (CRC Press, New York, 1997).

²Y. C. Su, L. W. Lin, and A. P. Pisano, *J. Microelectromech. Syst.* **11**, 736 (2002).

³X. Zhu and E. S. Kim, *Sens. Actuators, A* **66**, 355 (1998).

⁴R. H. Baughman, C. Cui, A. A. Zakhidov, Z. Iqbal, J. N. Barisci, G. M. Spinks, G. G. Wallace, A. Mazzoldi, D. De Rossi, A. G. Rinzler, O. Jaszchinski, S. Roth, and M. Kertesz, *Science* **284**, 1340 (1999).

⁵S. Juodkazis, N. Mukai, R. Wakai, A. Yamaguchi, S. Matsuo, and H. Misawa, *Nature (London)* **408**, 178 (2000).

⁶B. Raguse, K.-H. Müller, and L. Wiczorek, *Adv. Mater. (Weinheim, Ger.)* **15**, 922 (2003).

⁷V. Balzani, M. Venturi, and A. Credi, *Molecular Devices and Machines—A Journey into the Nanoworld* (Wiley-VCH, Weinheim, 2003).

⁸H.-R. Tseng, S. A. Vignon, and J. F. Stoddart, *Angew. Chem., Int. Ed.* **42**, 1491 (2003).

⁹R. Ballardini, V. Balzani, A. Credi, M. T. Gandolfi, and M. Venturi, *Acc. Chem. Res.* **34**, 445 (2001).

¹⁰H.-R. Tseng, D. Wu, N. Fang, X. Zhang, and J. F. Stoddart, *ChemPhysChem* **5**, 111 (2004).

¹¹T. J. Huang, H.-R. Tseng, L. Sha, W. Lu, B. Brough, A. H. Flood, B.-D. Yu, P. C. Celestre, J. P. Chang, J. F. Stoddart, and C.-M. Ho, *Nano Lett.* (to be published).

¹²M. Jiménez, C. Dietrich-Buchecker, and J.-P. Sauvage, *Angew. Chem., Int. Ed.* **39**, 3284 (2000).

¹³See EPAPS Document No.E-APPLAB-85-020448 for a full description of molecular modeling studies, molecular force calculations, beam bending calculations, and control experiments. A direct link to this document may be found in the online article's HTML reference section. The document may also be reached via the EPAPS homepage (<http://www.aip.org/pubservs/epaps.html>) or from <ftp.aip.org> in the directory/epaps/. See the EPAPS homepage for more information.

¹⁴We are aware that the disulfide tether or the underlying gold atoms to which they are attached might be migrating within each cycle.